

Dacian N. Daescu^{1*}, I. Michael Navon²

¹Portland State University, Portland, Oregon, ²Florida State University, Tallahassee, Florida

1. INTRODUCTION

Observation sensitivity techniques have been initially developed in the context of 3D-Var data assimilation for applications to targeted observations (Baker and Daley 2000, Doerenbecher and Bergot 2001). Adjoint-based methods are currently implemented in NWP to monitor the observation impact on analysis and short-range forecasts (Fourrié et al. 2002, Langland and Baker 2004, Zhu and Gelaro 2008).

An optimal use of the time-distributed observational data may be achieved with a four dimensional variational data assimilation system (4D-Var DAS) and the adjoint methodology may be used to estimate the forecast sensitivity with respect to all parameters in the DAS. Specification of the statistical properties of the background and observation errors is a key DAS ingredient and accurate error estimates are often difficult to provide. A better understanding of how uncertainties in the specification of the error statistics will impact the analysis and forecast may be achieved by extending the sensitivity analysis to the DAS input $[\mathbf{y}, \mathbf{R}, \mathbf{x}_b, \mathbf{B}]$. The error-covariance sensitivity analysis may be used to identify the observation and background components where improved statistical information would be of most benefit.

In this work the forecast sensitivity with respect to the time-series of data/error covariance pairs $(\mathbf{y}_i, \mathbf{R}_i), i = 0, 1, \dots, N$ and to the background input pair $(\mathbf{x}_b, \mathbf{B})$ in a 4D-Var DAS is presented and the close relationship between the sensitivities within each pair is discussed. In practical applications a high computational cost is required to provide accurate observation sensitivity estimates since the linear algebra involves Hessian of the 4D-Var cost functional. To overcome this difficulty, a reduced-order observation sensitivity approach is formulated

by projection on a low-dimensional state subspace. An optimal basis to the reduced space is shown to be closely related to the Hessian singular vectors optimized at the observation time. A computationally feasible method is proposed to identify a projection operator on a low-dimensional control space that incorporates in a consistent fashion information pertinent to the 4D-Var data assimilation procedure and to the forecast sensitivity. Idealized twin experiments are performed with a Lin-Rood finite volume global shallow-water model (Lin and Rood 1997) and initial conditions from ECMWF ERA-40 data sets. A nonlinear 4D-Var assimilation scheme is implemented using first and second order adjoint modeling to provide gradient and Hessian information, respectively. Preliminary numerical results and a comparative analysis with observation sensitivities evaluated in the full model space indicate that the reduced-order approach may be used to achieve significant computational savings in the observation sensitivity estimation. Limitations of the current implementation and future research directions are also discussed.

2. 4D-VAR FORECAST SENSITIVITY

A general framework to sensitivity analysis in the context of optimal control is discussed by Le Dimet et al. (1997). Corresponding to the 4D-Var cost functional

$$\begin{aligned} \mathcal{J}(\mathbf{x}_0) &= \frac{1}{2}(\mathbf{x}_0 - \mathbf{x}_b)^T \mathbf{B}^{-1}(\mathbf{x}_0 - \mathbf{x}_b) \\ &+ \frac{1}{2} \sum_{i=0}^N (H_i(\mathbf{x}_i) - \mathbf{y}_i)^T \mathbf{R}_i^{-1} (H_i(\mathbf{x}_i) - \mathbf{y}_i) \\ \mathbf{x}_0^a &= \text{Arg min } \mathcal{J} \end{aligned} \quad (1)$$

the optimality condition $\nabla_{\mathbf{x}_0} \mathcal{J}(\mathbf{x}_0^a) = 0$ is

$$\begin{aligned} 0 &= \mathbf{B}^{-1}(\mathbf{x}_0^a - \mathbf{x}_b) \\ &+ \sum_{i=0}^N \mathbf{M}_{0,i}^T \mathbf{H}_i^T \mathbf{R}_i^{-1} (H_i(\mathbf{x}_i) - \mathbf{y}_i) \end{aligned} \quad (2)$$

where $\mathbf{M}_{0,i}(\mathbf{x}_0^a)$ is the tangent linear model associated to the nonlinear model integration $\mathbf{x}_i =$

* *Corresponding author address:* Dacian N. Daescu, Department of Mathematics and Statistics, Portland State University, P.O. Box 751, Portland, OR 97207, USA; e-mail: daescu@pdx.edu

$\mathcal{M}_{t_0 \rightarrow t_i}(\mathbf{x}_0^a)$ and $\mathbf{H}_i(\mathbf{x}_i)$ is the Jacobian matrix of the observation operator H_i evaluated at \mathbf{x}_i . An analytic derivation of the 4D-Var DAS sensitivity equations from the first order necessary condition is provided by Daescu (2008). The sensitivity equations of a scalar aspect $J^v(\mathbf{x}_v)$ of the forecast $\mathbf{x}_v = \mathcal{M}_{t_0 \rightarrow t_v}(\mathbf{x}_0^a)$ are given in Table 1

Table 1: Forecast sensitivity to 4D-Var DAS input.

| DAS input | Forecast sensitivity (∇J^v) |
|------------------|--|
| \mathbf{y}_i | $\mathbf{R}_i^{-1} \mathbf{H}_i \mathbf{M}_{0,i} \mathbf{A} \nabla_{\mathbf{x}_0^a} J^v$ |
| σ_i^2 | $(\mathbf{R}_i^{-1} (H_i(\mathbf{x}_i) - \mathbf{y}_i)) \circ \nabla_{\mathbf{y}_i} J^v$ |
| \mathbf{R}_i : | $(\mathbf{R}_i^{-1} (H_i(\mathbf{x}_i) - \mathbf{y}_i)) \otimes \nabla_{\mathbf{y}_i} J^v$ |
| \mathbf{x}_b | $\mathbf{B}^{-1} \mathbf{A} \nabla_{\mathbf{x}_0^a} J^v$ |
| σ_b^2 | $(\mathbf{B}^{-1} (\mathbf{x}_0^a - \mathbf{x}_b)) \circ \nabla_{\mathbf{x}_b} J^v$ |
| \mathbf{B} : | $(\mathbf{B}^{-1} (\mathbf{x}_0^a - \mathbf{x}_b)) \otimes \nabla_{\mathbf{x}_b} J^v$ |

where \otimes and \circ denote the Kronecker and Hadamard product, respectively, $(:)$ denotes the vec operator that transforms a matrix into a column vector (Magnus and Neudecker 1999) and \mathbf{A} denotes the inverse Hessian matrix at the analysis \mathbf{x}_0^a

$$\mathbf{A} \stackrel{def}{=} [\nabla_{\mathbf{x}_0 \mathbf{x}_0}^2 \mathcal{J}(\mathbf{x}_0^a)]^{-1} \quad (3)$$

The sensitivity calculations require the solution to the linear system

$$\mathbf{A}^{-1} \boldsymbol{\mu}_0 = \nabla_{\mathbf{x}_0^a} J^v \quad (4)$$

involving the 4D-Var Hessian and an iterative procedure such as the conjugate gradient method (CG) must be used to approximate the solution $\boldsymbol{\mu}_0$ to the system (4). For time distributed observations, the errors in the estimation of $\boldsymbol{\mu}_0$ are further propagated into the observation sensitivity computations by the tangent linear model $\mathbf{M}_{0,i}$. An increased accuracy in the numerical solution to (4) is thus necessary for the sensitivity estimates to be reliable.

It is noticed that if the observation errors are assumed to be uncorrelated, $\mathbf{R}_i = \text{diag}(\sigma_{i,1}^2, \dots, \sigma_{i,k_i}^2)$, the sensitivity to the observation-error variance is

$$\frac{\partial J^v}{\partial \sigma_{i,j}^2} = \frac{1}{\sigma_{i,j}^2} (H_i(\mathbf{x}_i) - \mathbf{y}_i)_j \frac{\partial J^v}{\partial (\mathbf{y}_i)_j}, \quad j = 1, 2, \dots, k_i \quad (5)$$

For each component $(\mathbf{y}_i)_j$ of the observational data vector \mathbf{y}_i at time t_i , the sensitivity to the observation-error variance $\sigma_{i,j}^2$ is related to the observation sensitivity by the *proportionality coefficient* $(H_i(\mathbf{x}_i) - \mathbf{y}_i)_j / \sigma_{i,j}^2$ - the analysis fit to data divided by the observation-error variance.

2.1 Low-rank approximation using HSVs

The forecast sensitivity with respect to the observational data set \mathbf{y}_i at time t_i may be expressed as

$$\nabla_{\mathbf{y}_i} J^v = \mathbf{R}_i^{-1} \mathbf{H}_i \mathbf{A}_i \nabla_{\mathbf{x}_i} J^v \quad (6)$$

where the matrix

$$\mathbf{A}_i = \mathbf{M}_{0,i} \mathbf{A} \mathbf{M}_{0,i}^T \quad (7)$$

is an approximation of the covariance matrix of the errors in \mathbf{x}_i . The Hessian singular vectors (HSVs) optimized at the observation time t_i are the generalized singular vectors of the pair $(\mathbf{M}_{0,i}, \mathbf{A}^{-1/2})$ and are obtained by solving a generalized eigenvalue problem

$$\mathbf{M}_{0,i}^T \mathbf{M}_{0,i} \mathbf{v}_j = \lambda_j \mathbf{A}^{-1} \mathbf{v}_j \quad (8)$$

HSVs are \mathbf{A}^{-1} -orthonormal and the evolved singular vectors $\mathbf{u}_j = (1/\sqrt{\lambda_j}) \mathbf{M}_{0,i} \mathbf{v}_j$ are orthonormal eigenvectors to \mathbf{A}_i :

$$\mathbf{A}_i \mathbf{u}_j = \lambda_j \mathbf{u}_j \quad (9)$$

Given $k < n$,

$$\mathbf{A}_i^{(k)} = \sum_{j=1}^k \lambda_j \mathbf{u}_j \mathbf{u}_j^T \quad (10)$$

provides an optimal rank- k approximation to \mathbf{A}_i in any unitarily invariant norm and may be used to estimate the observation sensitivities

$$\nabla_{\mathbf{y}_i} J^v \approx \mathbf{R}_i^{-1} \mathbf{H}_i \mathbf{A}_i^{(k)} \nabla_{\mathbf{x}_i} J^v \quad (11)$$

The solution to the generalized eigenvalue problem (8) may be obtained through an iterative algorithm that requires only matrix-vector products such as the Jacobi-Davidson method (Sleijpen and Van der Vorst 1996). An exact evaluation of the required Hessian-vector products may be obtained with a second order adjoint model (SOA) (Le Dimet et al. 2002). Gradient differences may be used to approximate $\mathbf{A}^{-1} \mathbf{v} \approx (\nabla \mathcal{J}(\mathbf{x}_0 + \epsilon \mathbf{v}) - \nabla \mathcal{J}(\mathbf{x}_0)) / \epsilon$ which is an exact relationship for a quadratic 4D-Var cost functional, e.g., in the incremental formulation (Courtier et al. 1994). For each observation time t_i a new set of HSVs must be computed and the computational cost increases as $t_i - t_0$ increases. The high computational burden associated to the HSVs is a major factor that has hampered their potential benefit in many practical applications. A computationally efficient approach is to solve the ordinary eigenvalue problem (9) using an approximation of the inverse Hessian matrix \mathbf{A} . Approximations based on the leading eigenvectors and the

BFGS method are discussed in the work of Fisher and Courtier (1995), Leutbecher (2003).

2.2 Reduced-order 4D-Var observation sensitivity

The sensitivity equations are derived from the optimality condition (2) whereas in the practical implementation the minimization (1) is terminated when the gradient satisfies a certain convergence criteria or simply after a prescribed number of iterations. To obtain an estimate of the observation sensitivity that is consistent to the data assimilation process, Zhu and Gelaro (2008) implemented the adjoint of the minimization algorithm in the GSI analysis scheme (Wu et al. 2002).

In this work a reduced-order approach to observation sensitivity is considered where information gathered in the 4D-Var minimization (1) is used to define an appropriate low-rank state subspace. In a general framework, the reduced-order 4D-Var is formulated by projecting $\delta \mathbf{x}_0 = \mathbf{x}_0 - \mathbf{x}_b$ onto a k -dimensional control space (Daescu and Navon 2008)

$$\mathbf{\Pi} \delta \mathbf{x}_0 = \mathbf{\Psi} \boldsymbol{\eta} = \sum_{i=1}^k \eta_i \boldsymbol{\psi}_i \quad (12)$$

where the matrix $\mathbf{\Psi} = [\boldsymbol{\psi}_1, \dots, \boldsymbol{\psi}_k] \in \mathcal{R}^{n \times k}$ has the reduced-space basis vectors as columns (orthonormal), $\mathbf{\Pi} = \mathbf{\Psi} \mathbf{\Psi}^T$ is the projection operator, and $\boldsymbol{\eta} = (\eta_1, \dots, \eta_k)^T \in R^k$ is the coordinates vector in the reduced space

$$\boldsymbol{\eta} = \mathbf{\Psi}^T \delta \mathbf{x}_0 \quad (13)$$

The reduced-order 4D-Var problem searches for the optimal coefficients $\boldsymbol{\eta}$

$$\hat{\mathcal{J}}(\boldsymbol{\eta}) := \mathcal{J}(\mathbf{x}_b + \mathbf{\Psi} \boldsymbol{\eta}); \quad \min_{\boldsymbol{\eta} \in R^k} \hat{\mathcal{J}}(\boldsymbol{\eta}) \quad (14)$$

If $\boldsymbol{\eta}^a$ is the solution to (14), an approximation to the analysis (1) is obtained as

$$\mathbf{x}_0^a \approx \mathbf{x}_b + \mathbf{\Psi} \boldsymbol{\eta}^a \quad (15)$$

It is noticed (Daescu and Navon 2007) that derivatives in the reduced space are evaluated according to

$$\nabla_{\boldsymbol{\eta}} \hat{\mathcal{J}} = \mathbf{\Psi}^T \nabla_{\mathbf{x}_0} \mathcal{J} \quad (16)$$

$$\nabla_{\boldsymbol{\eta}}^2 \hat{\mathcal{J}} = \mathbf{\Psi}^T [\nabla_{\mathbf{x}_0 \mathbf{x}_0}^2 \mathcal{J}] \mathbf{\Psi} \quad (17)$$

such that in the reduced-space the linear system (4) becomes

$$\mathbf{\Psi}^T \mathbf{A}^{-1} \mathbf{\Psi} \hat{\boldsymbol{\mu}}_0 = \mathbf{\Psi}^T \nabla_{\mathbf{x}_0^a} J^v \quad (18)$$

The reduced Hessian matrix $\mathbf{\Psi}^T \mathbf{A}^{-1} \mathbf{\Psi} \in \mathcal{R}^{k \times k}$ is positive definite, provided that \mathbf{A}^{-1} is positive definite, and the reduced-order approach estimates the observation sensitivity according to

$$\nabla_{\mathbf{y}_i} J^v \approx \mathbf{R}_i^{-1} \mathbf{H}_i \mathbf{M}_{0,i} \mathbf{\Psi} \hat{\boldsymbol{\mu}}_0 \quad (19)$$

Remark 1: It is noticed from (18) that $\mathbf{\Psi} \hat{\boldsymbol{\mu}}_0$ is a solution to the projected system (4)

$$\mathbf{\Pi} \mathbf{A}^{-1} \mathbf{\Psi} \hat{\boldsymbol{\mu}}_0 = \mathbf{\Pi} \nabla_{\mathbf{x}_0^a} J^v \quad (20)$$

and that if the approximation (15) is exact, then the reduced-order 4D-Var observation sensitivity estimate relies on the reduced-rank approximation to the inverse Hessian matrix

$$\mathbf{A} \approx \mathbf{\Psi} \left[\mathbf{\Psi}^T \mathbf{A}^{-1} \mathbf{\Psi} \right]^{-1} \mathbf{\Psi}^T \quad (21)$$

2.3 Reduced-order subspace selection

In practice the 4D-Var minimization (1) is implemented by performing k -iterations

$$\mathbf{x}_0^{(i+1)} = \mathbf{x}_0^{(i)} + \alpha_i \mathbf{d}^{(i)}, \quad i = 0, 1, \dots, k-1 \quad (22)$$

with the initial guess $\mathbf{x}_0^{(0)} = \mathbf{x}_b$ and the optimality condition (2) is only approximately satisfied. The analysis \mathbf{x}_0^a is expressed

$$\mathbf{x}_0^a = \mathbf{x}_b + \sum_{i=0}^{k-1} \alpha_i \mathbf{d}^{(i)} \quad (23)$$

and the analysis increment $\delta \mathbf{x}_0^a$ is an element of the vector space spanned by the descent directions $\delta \mathbf{x}_0^a \in \mathcal{S} = \text{Span}\{\mathbf{d}^{(0)}, \mathbf{d}^{(1)}, \dots, \mathbf{d}^{(k-1)}\}$.

Remark 2: If the conjugate gradient or the BFGS method is implemented and the cost functional (1) is quadratic (e.g., incremental 4D-Var formulation) then \mathbf{x}_0^a is the minimizer of \mathcal{J} over the set $\{\mathbf{x}_b + \mathcal{S}\}$. Denoting $\{\boldsymbol{\psi}_0, \dots, \boldsymbol{\psi}_{k-1}\}$ an orthonormal basis to \mathcal{S} , $\nabla_{\boldsymbol{\eta}} \hat{\mathcal{J}}(\boldsymbol{\eta}^a) = 0$ and the optimality condition is satisfied in the reduced space, although in general $\nabla_{\mathbf{x}_0} \mathcal{J}(\mathbf{x}_0^a) \neq 0$. The reduced-space is thus consistent to the 4D-Var minimization process and the approximation (15) is exact.

An additional enhancement is obtained by appending to the reduced basis the unit vector $\boldsymbol{\psi}_k$ orthogonal to each of $\boldsymbol{\psi}_0, \dots, \boldsymbol{\psi}_{k-1}$, $\boldsymbol{\psi}_k \in \{\boldsymbol{\psi}_0, \dots, \boldsymbol{\psi}_{k-1}\}^\perp$, such that $\nabla_{\mathbf{x}_0^a} J^v \in \text{Span}\{\boldsymbol{\psi}_0, \dots, \boldsymbol{\psi}_{k-1}, \boldsymbol{\psi}_k\}$. The reduced-space provides thus an exact representation of the forecast

sensitivity to analysis $\mathbf{\Pi} \nabla_{\mathbf{x}_0^a} J^v = \nabla_{\mathbf{x}_0^a} J^v$ and an error estimate may be derived from Eqs. (4) and (20)

$$\boldsymbol{\mu}_0 - \boldsymbol{\Psi} \hat{\boldsymbol{\mu}}_0 = (\mathbf{A} \boldsymbol{\Pi} \mathbf{A}^{-1} - \mathbf{I}) \boldsymbol{\Psi} \hat{\boldsymbol{\mu}}_0 \quad (24)$$

where \mathbf{I} is the $n \times n$ identity matrix.

3. NUMERICAL EXPERIMENTS

Numerical experiments are setup with a finite volume global shallow-water (SW) model of Lin and Rood (1997) at a resolution of $2.5^\circ \times 2.5^\circ$ and with a time step $\Delta t = 600\text{s}$. The state vector $\mathbf{x} = (h, u, v)$ where h is the geopotential height and u and v are the zonal and meridional wind velocities, respectively. An idealized 4D-Var DAS is considered in the twin experiments framework: a reference initial state \mathbf{x}_0^t (“the truth”) is taken from the European Centre for Medium-Range Weather Forecasts (ECMWF) ERA-40 500 hPa data valid for 0600 UTC 15 March 2002; the background estimate \mathbf{x}_b to \mathbf{x}_0^t is obtained from a 6h integration of the SW model initialized at $t_0 - 6\text{h}$ with ECMWF ERA-40 500 hPa data valid for 0000 UTC 15 March 2002. “Observational data” for the assimilation procedure is generated from a model trajectory initialized with \mathbf{x}_0^t and corrupted with random errors from a normal distribution $N(0, \sigma^2)$. The standard deviation is chosen $\sigma_h = 5\text{ m}$ for the height and $\sigma_u = \sigma_v = 0.5\text{ m s}^{-1}$ for the velocities and the observation errors are assumed to be uncorrelated. The background errors are assumed uncorrelated and are specified at a ratio $\sigma_b^2/\sigma^2 = 4$ to the observations. Data sets are provided at locations shown in Fig. 1 at a time increment of one hour over the data assimilation interval $[t_0, t_0 + 6\text{h}]$.

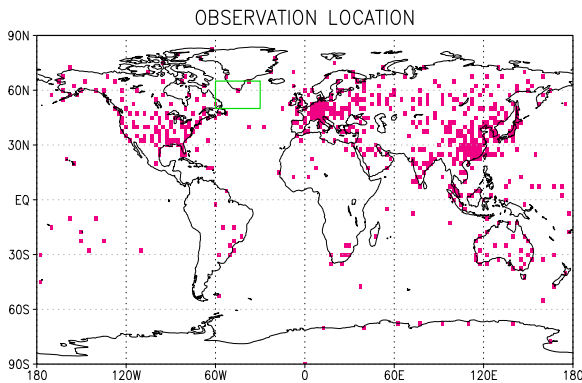


Figure 1: Observation locations and the verification domain at $t_v = t_0 + 30\text{h}$.

The observation locations were obtained from the

actual locations of the radiosondes observations in a realistic data assimilation system projected to the closest model grid point. The observation operator H is thus a matrix with entries 0 and 1 only and there are 572 observation locations.

At the verification time $t_v = t_0 + 30\text{h}$ we consider as reference state $\mathbf{x}_v^t = \mathcal{M}_{t_0 \rightarrow t_v}(\mathbf{x}_0^t)$ and the forecast $\mathbf{x}_v^f = \mathcal{M}_{t_0 \rightarrow t_v}(\mathbf{x}_0^a)$. The forecast error is displayed in Fig. 2 using a total energy norm to obtain grid-point values (units of $\text{m}^2 \text{s}^{-2}$). The verification domain is taken $\mathcal{D}_v = [50^\circ N, 65^\circ N] \times [60^\circ W, 30^\circ W]$ and the functional J^v is defined as the forecast error over \mathcal{D}_v in a total energy metric

$$J^v = (\mathbf{x}_v^f - \mathbf{x}_v^t)^T \mathbf{P}^T \mathbf{E} \mathbf{P} (\mathbf{x}_v^f - \mathbf{x}_v^t) \quad (25)$$

where \mathbf{P} is the projection operator on \mathcal{D}_v .

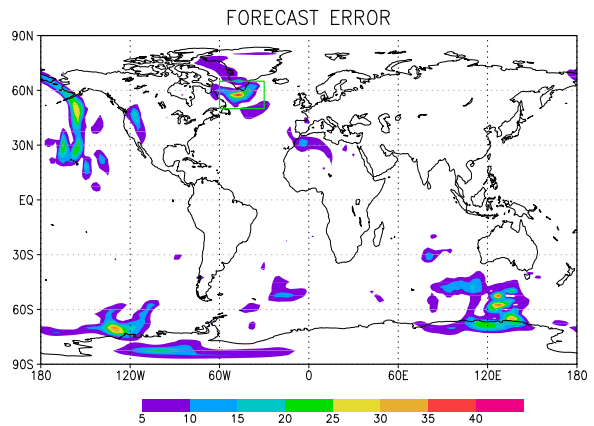


Figure 2: Forecast error ($\text{m}^2 \text{s}^{-2}$) at $t_v = t_0 + 30\text{h}$ and selection of the verification domain.

3.1 Observation-sensitivity analysis

The observation sensitivity analysis reveals that the specified forecast aspect J^v exhibits a large sensitivity with respect to only a few of the observations in the DAS. As a measure of the forecast sensitivity to observation and error variance at each data location over the assimilation time interval we consider the time cumulative magnitude of the sensitivities $\sum_{i=0}^N |\nabla_{\mathbf{y}_i} J^v|$ and $\sum_{i=0}^N |\nabla_{\sigma_i^2} J^v|$, respectively. The location of the observations and error variances of largest forecast sensitivity is displayed in Fig. 3 for each of u , v , and h data. A distinct configuration and magnitude is noticed for each data component, indicating that the location of observations and error variances that provide a potentially large forecast impact depends on the data type.

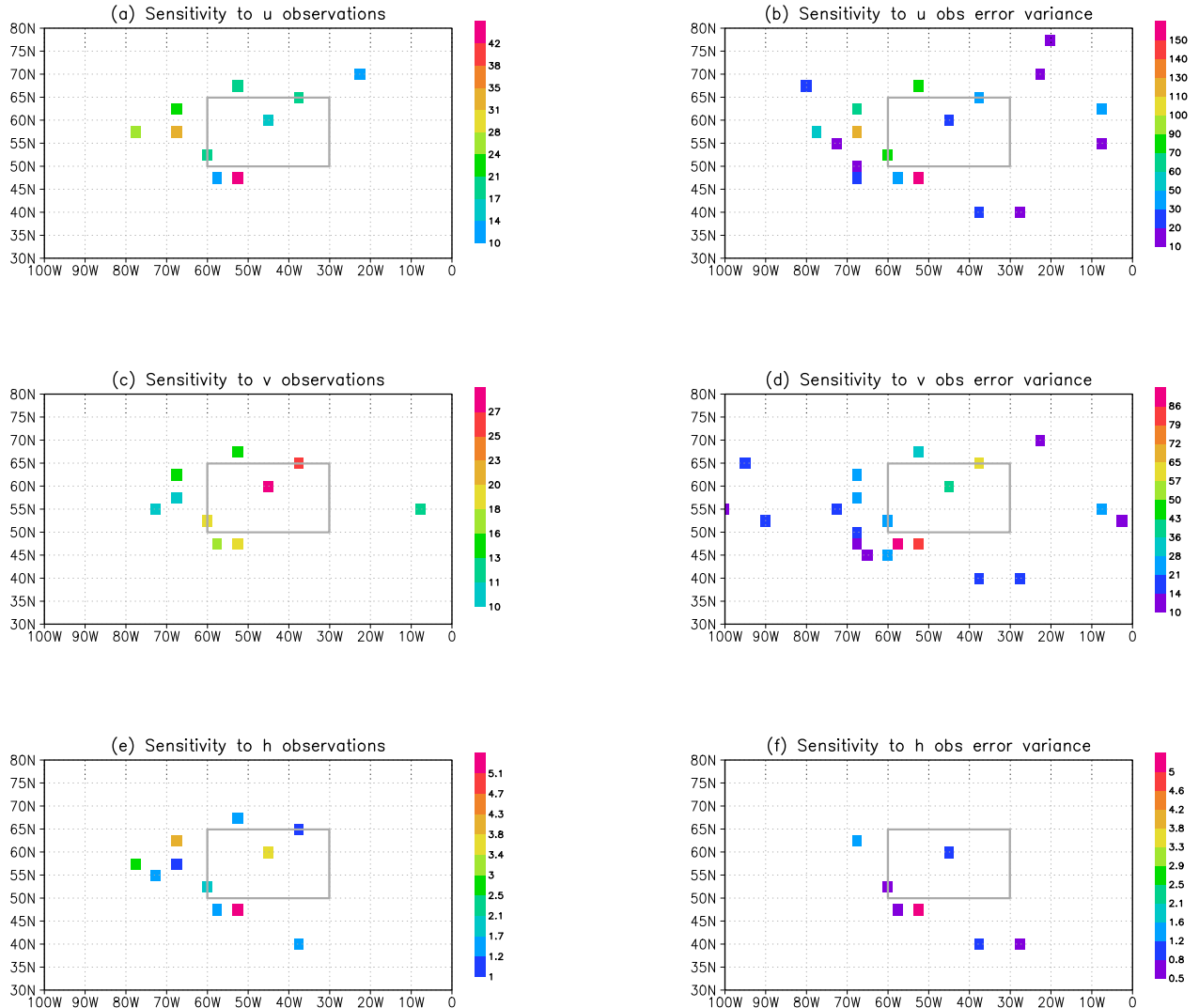


Figure 3: Locations of data with forecast sensitivity of largest magnitude. Time cumulative magnitudes of the observation and error-variance sensitivities are displayed.

Evaluation of the observation sensitivity in the full state space requires the solution to the large-scale linear system (4), whereas a low-dimensional system (18) is solved in the reduced-order approach. A second order adjoint model (SOA) has been used to provide the Hessian-vector products required in the CG iteration. The reduced-order approach entailed significant computational savings and a reduction of as much as 75% in the CPU time using a reduced-space of dimension $k = 100$. The velocity components of the full state solution μ_0 and the corresponding reduced order approximation $\Psi\hat{\mu}_0$ are displayed in Fig. 4. It is noticed that the reduced order approach is able to closely match the “shape” of the solution, however the amplitude of the solution components is in general lower. To illustrate this aspect, in Fig. 5 we further provide the velocity com-

ponents of the full state solution μ_0 and the reduced order solution $\Psi\hat{\mu}_0$ corresponding a global forecast error aspect ($\mathcal{D}_v = [90^\circ S, 90^\circ N] \times [180^\circ W, 180^\circ E]$). A comparison of the observation sensitivity estimates in the full space to the reduced-order estimates indicates that the reduced-order approach is able to properly identify the data locations of largest sensitivity magnitude. Illustrative results are shown in Fig. 6 and Fig. 7 for u -wind data at $t = 6$ h corresponding to $\mathcal{D}_v = [50^\circ N, 65^\circ N] \times [60^\circ W, 30^\circ W]$ and $\mathcal{D}_v = [90^\circ S, 90^\circ N] \times [180^\circ W, 180^\circ E]$, respectively. The results also indicate that the observation sensitivity estimates in the reduced-order approach have larger magnitudes as compared to the full state estimates.

From Table 1 it is noticed that the sensitivity to

the background is evaluated according to $\nabla_{\mathbf{x}_b} J^v = \mathbf{B}^{-1} \boldsymbol{\mu}_0$. Since in our experiments \mathbf{B} is taken to be a diagonal matrix, $\boldsymbol{\mu}_0$ represents the sensitivity to background multiplied by the background-error variance, $\boldsymbol{\mu}_0 = \sigma_b^2 \circ \nabla_{\mathbf{x}_b} J^v$. The reduced order ap-

proach is thus able to properly identify the locations of high background and observation sensitivity, however it provides lower background sensitivity values and higher observation sensitivity values, as compared to the full state estimates.

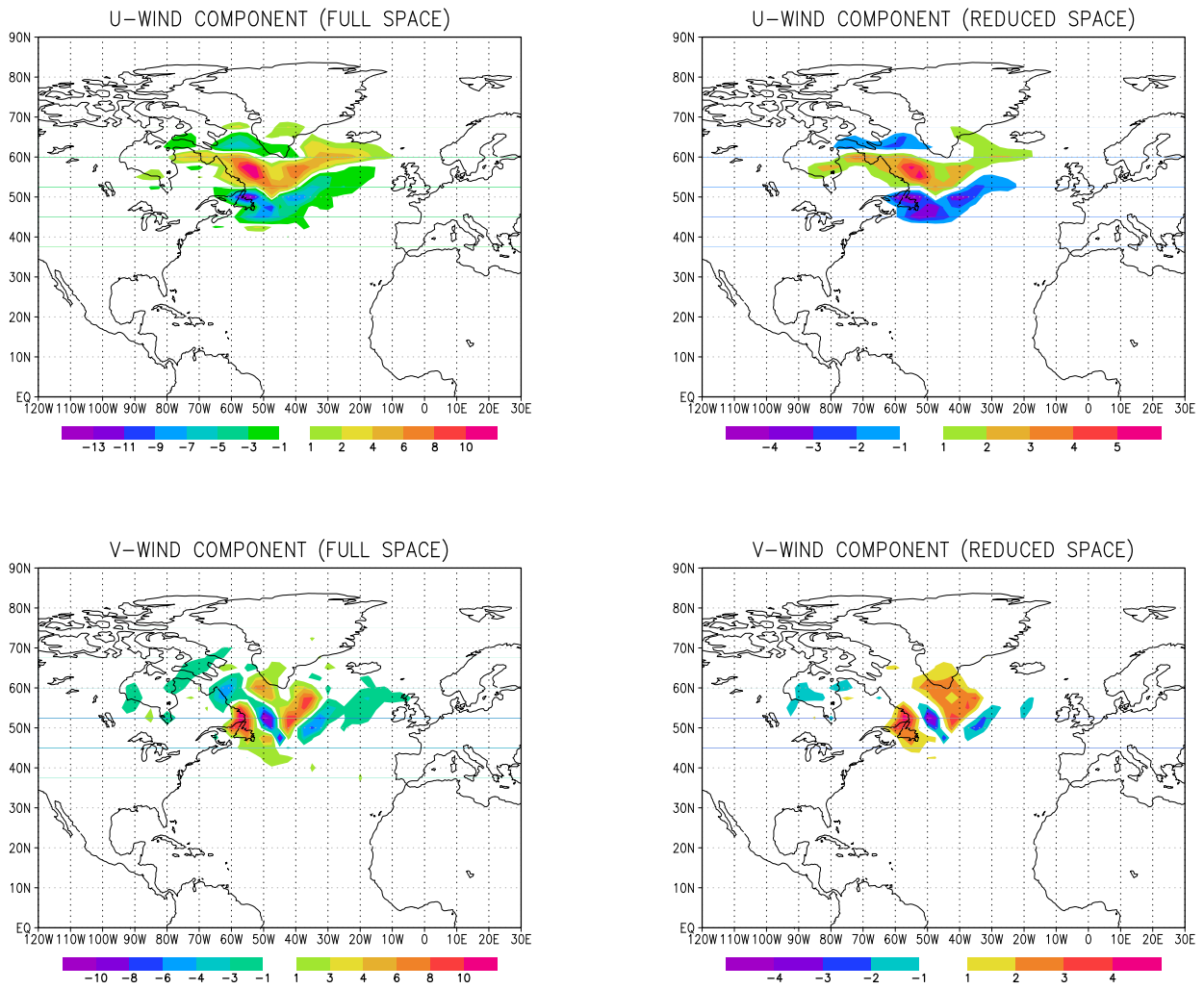


Figure 4: The velocity components of the full state solution $\boldsymbol{\mu}_0$ and the corresponding reduced order approximation $\Psi \hat{\boldsymbol{\mu}}_0$. The forecast error J^v is defined over the verification domain $[50^\circ N, 65^\circ N] \times [60^\circ W, 30^\circ W]$.

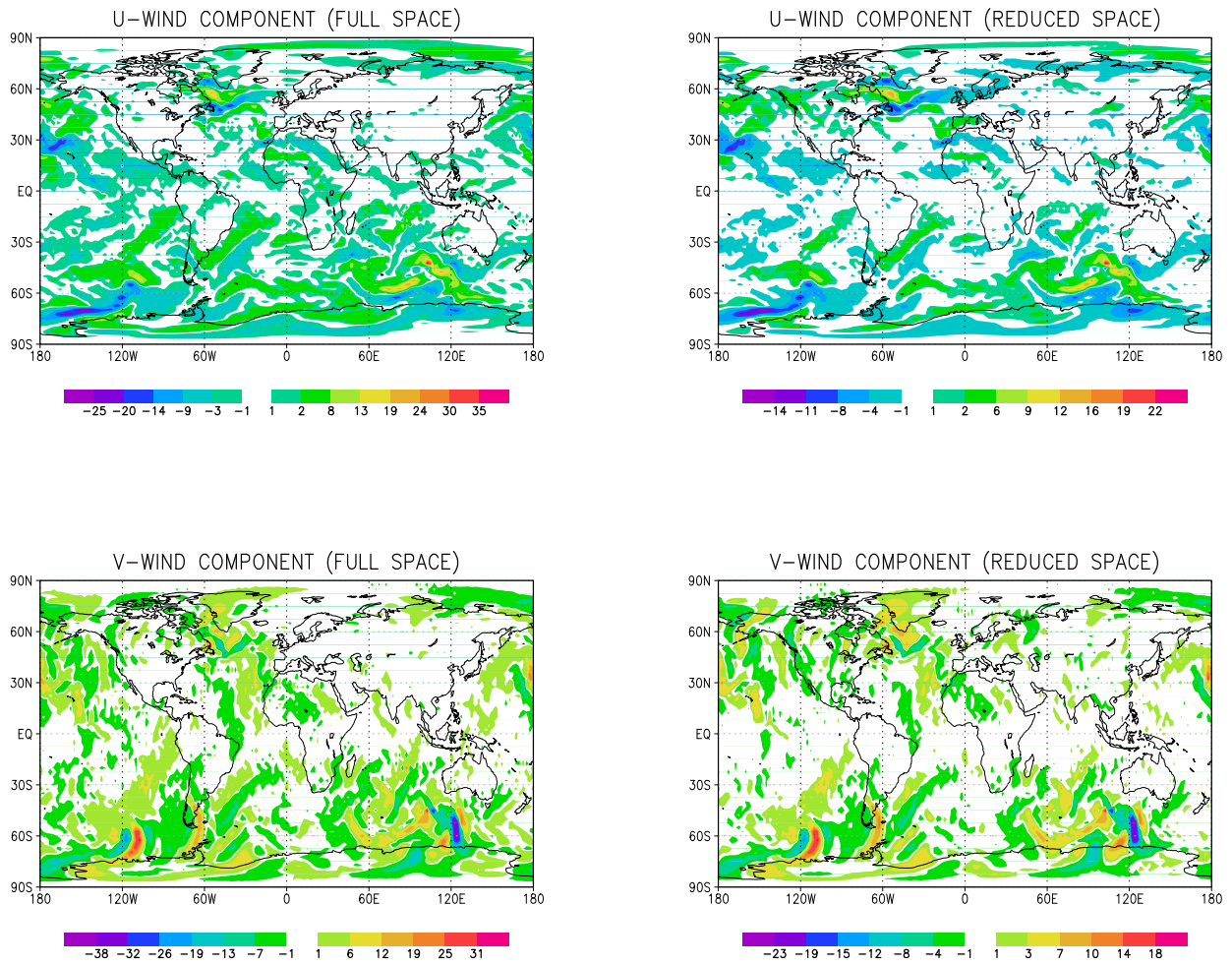


Figure 5: The velocity components of the full state solution μ_0 and the corresponding reduced order approximation $\Psi\hat{\mu}_0$ for a forecast aspect J^v defined over the entire domain.

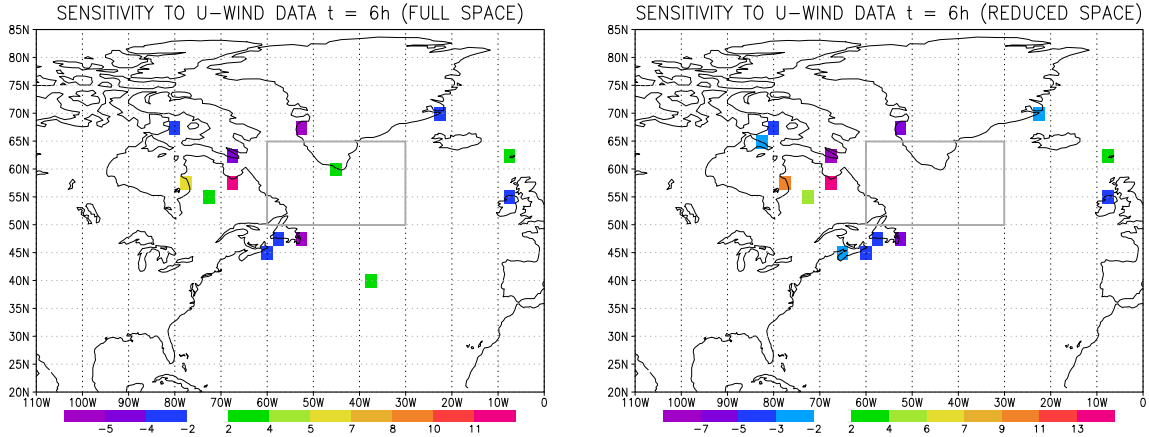


Figure 6: Data locations of largest sensitivity magnitude at $t - t_0 = 6$ h for the forecast error defined over the verification domain $\mathcal{D}_v = [50^\circ N, 65^\circ N] \times [60^\circ W, 30^\circ W]$.

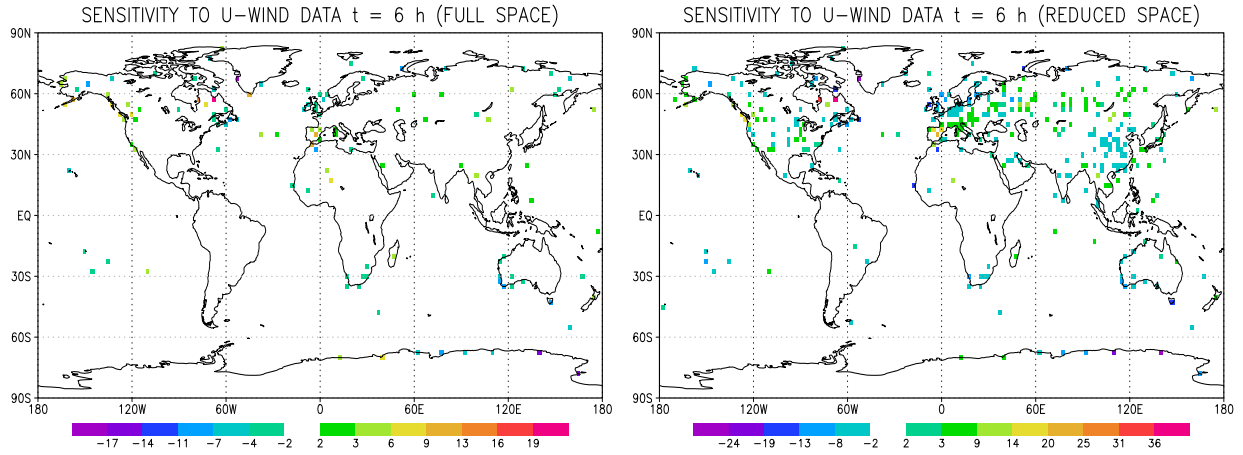


Figure 7: Data locations of largest sensitivity magnitude at $t - t_0 = 6$ h for a global forecast error $\mathcal{D}_v = [90^\circ S, 90^\circ N] \times [180^\circ W, 180^\circ E]$.

4. CONCLUDING REMARKS

The 4D-Var sensitivity analysis involves a significant software development and several simplifying assumptions are required in NWP applications to reduce the computational burden. In this study a general framework to reduced-order observation sensitivity is presented as a computationally feasible approach to practical applications. Identification of a reduced-order space based on the information accumulated during the 4D-Var minimization process requires little additional computational effort and software development. The simplicity of the SW

model allowed the implementation of a second order adjoint model associated to the nonlinear 4D-Var formulation and numerical estimation of the sensitivities in both full and reduced-order space. Idealized 4D-Var observation sensitivity experiments indicate that the reduced-order approach is able to properly identify data sets and observation locations of largest forecast sensitivity while providing significant computational savings. If an increased accuracy in the observation sensitivity estimates is required, the reduced-order approach may be used to provide an efficient initial guess to the full state sensitivity estimation. Further applications to adaptive

data thinning and targeted observations are envisaged and valuable insight may be gained through observing system simulation experiments (OSSE's). The 4D-Var framework allows a sensitivity analysis with respect to time-space distributed data and it is well suited for applications that involve multiple observation targeting instants in the assimilation window e.g., flight path design.

Acknowledgements

This research was supported by NASA Modeling, Analysis and Prediction Program under award No. NNG06GC67G.

References

- Atlas, R., 1997: Atmospheric observations and experiments to assess their usefulness in data assimilation. *J. Meteorol. Soc. Japan*, **75**, No. 1B, 111–130.
- Baker, N.L., and R. Daley, 2000: Observation and background adjoint sensitivity in the adaptive observation-targeting problem. *Q.J.R. Meteorol. Soc.*, **126**, 1431–1454.
- Courtier, P., Thepaud, J.N., and A. Hollingsworth, 1994: A strategy of operational implementation of 4D-Var using an incremental approach. *Q.J.R. Meteorol. Soc.* **120**, 1367–1388.
- Daescu, D.N., 2008: On the sensitivity equations of 4D-Var data assimilation. *Mon. Wea. Rev.*, in press.
- Daescu, D.N., and I.M. Navon, 2007: Efficiency of a POD-based reduced second order adjoint model in 4D-Var data assimilation. *Int. J. Num. Meth. Fluids*, **53**, 985–1004.
- Daescu, D.N., and I.M. Navon, 2008: A dual-weighted approach to order reduction in 4D-VAR data assimilation *Mon. Wea. Rev.*, in press.
- Doerenbecher, A., and T. Bergot, 2001: Sensitivity to observations applied to FASTEX cases. *Non. Proc. Geophys.*, **8**, 467–481.
- Fisher, M., and P. Courtier, 1995: Estimating the covariance matrices of analysis and forecast error in variational data assimilation. *ECMWF Tech. Memo.* **220**. European Centre for Medium-range Weather Forecasts (ECMWF), Reading, UK.
- Fourrié, N., A. Doerenbecher, T. Bergot, and A. Joly, 2002: Adjoint sensitivity of the forecast to TOVS observations. *Q.J.R. Meteorol. Soc.* **128**, 2759–2777.
- Langland, R.H., and N.L. Baker, 2004: Estimation of observation impact using the NRL atmospheric variational data assimilation adjoint system. *Tellus*, **56A**, 189–203.
- Le Dimet, F.-X., H.-E. Ngodock, and B. Luong, 1997: Sensitivity analysis in variational data assimilation. *J. Meteorol. Soc. Japan*, **75** (1B), 245–255.
- Le Dimet, F.X., I.M. Navon, and D.N. Daescu, 2002: Second order information in data assimilation. *Mon. Wea. Rev.*, **130** (3), 629–648.
- Leutbecher, M., 2003: A reduced rank estimate of forecast error variance changes due to intermittent modifications of the observing network. *J. Atmos. Sci.*, **60**, 729–742.
- Lin, S.-J., and R.B. Rood, 1997: An explicit flux-form semi-Lagrangian shallow-water model on the sphere. *Q.J.R. Meteorol. Soc.*, **123**, 2477–2498.
- Magnus, J.R., and H. Neudecker, 1999: *Matrix Differential Calculus with Applications in Statistics and Econometrics (Revised Edition)*. John Wiley & Sons Ltd., 395pp.
- Sleijpen, G.L.G., and van der Vorst, H.A., 1996: A Jacobi-Davidson iteration method for linear eigenvalue problems. *SIAM J. Matrix Anal. Appl.*, **17**(2), 401–425.
- Wu, W., R.J. Purser, and D.F. Parrish, 2002: Three dimensional variational analysis with spatially inhomogeneous covariances. *Mon. Wea. Rev.*, **130**, 2905–2916.
- Zhu, Y., and R. Gelaro, 2008: Observation sensitivity calculations using the adjoint of the Gridpoint Statistical Interpolation (GSI) analysis system. *Mon. Wea. Rev.*, in press.